HHS Public Access

Author manuscript

Biometals. Author manuscript; available in PMC 2019 March 08.

Published in final edited form as:

Biometals. 2018 August ; 31(4): 585–593. doi:10.1007/s10534-018-0107-5.

CatroxMP-II: a heme-modulated fibrinogenolytic metalloproteinase isolated from *Crotalus atrox* venom

Montamas Suntravat,
Department of Chemistry, National Natural Toxins Research Center, Texas A&M University-Kingsville, Kingsville, TX, USA

Paul R. Langlais,
The Department of Medicine, Division of Endocrinology, University of Arizona College of Medicine, Tucson, AZ, USA

Elda E. Sánchez, and
Department of Chemistry, National Natural Toxins Research Center, Texas A&M University-Kingsville, Kingsville, TX, USA

Vance G. Nielsen
The Department of Anesthesiology, University of Arizona College of Medicine, P.O. Box 245114, 1501 North Campbell Avenue, Tucson, AZ 85724-5114, USA, vgnielsen333@gmail.com

Abstract

It has been recently demonstrated that the hemotoxic venom activity of several species of snakes can be inhibited by carbon monoxide (CO) or a metheme forming agent. These and other data suggest that the biometal, heme, may be attached to venom enzymes and may be modulated by CO. A novel fibrinogenolytic metalloproteinase, named CatroxMP-II, was isolated and purified from the venom of a *Crotalus atrox* viper, and subjected to proteolysis and mass spectroscopy. An ion similar to the predicted singly charged m/z of heme at 617.18 was identified. Lastly, CORM-2 (tricarbonyldichlororuthenium (II) dimer, a CO releasing molecule) inhibited the fibrinogenolytic effects of CatroxMP-II on coagulation kinetics in human plasma. In conclusion, we present the first example of a snake venom metalloproteinase that is heme-bound and CO-inhibited.

Keywords

Snake venom metalloproteinase; Heme; Mass spectrometry; Carbon monoxide; Thrombelastography

Introduction

It has been recently demonstrated that the hemotoxic venom activity of several species of snakes can be inhibited in vitro and in vivo by exposure to carbon monoxide (CO) via

Correspondence to: Vance G. Nielsen.

Compliance with ethical standards

Conflict of interest The authors have no conflicts of interest.

thrombelastography (Nielsen 2018; Nielsen and Bazzell 2016, 2017; Nielsen et al. 2016, 2018a, b; Nielsen and Losada 2017; Nielsen and Matika 2017). Also of interest, an agent that causes metheme formation (Nielsen et al. 2011a) used to identify fibrinogen as a heme binding protein (Nielsen et al. 2011b) was demonstrated to decrease the prothrombotic activity of *Oxyuranus microlepidotus* venom (Nielsen et al. 2018a). While it was originally posited that CO may have inhibited snake venom metalloproteinase (SVMP) activity by in some way interacting with the typically zinc metal catalytic center, subsequent inactivation of a snake venom serine protease (SVSP) activity by CO could not be similarly explained (Nielsen and Bazzell 2017). Lastly, the CO concentration-coagulation kinetic response of the fibrinogenolytic venom of *Crotalus atrox* was sigmoidal in nature (Nielsen and Bazzell 2016). An example of this can be observed in Fig. 1, wherein unpublished data generated in this work (Nielsen and Bazzell 2016) demonstrate that the inhibition or venom mediated prolongation to reaction time (R, time to commence coagulation) is inhibited by a CO-releasing molecule in a sigmoidal fashion. Given that carboxyheme and metheme states inhibited both SVMP and SVSP, and that the concentration effects of CO on the inhibition of SVMP activity could be described as sigmoidal, a new hypothesis was formulated wherein a common, modulatory molecule bound to the various SVMPs and SVSPs was the ligand responsible for CO mediated inhibition; that molecule was heme.

While attractive, testing the hypothesis of heme as a molecule regulating SVMP and SVSP activity was problematic. Given that raw venom often contains multiple SVMPs and SVSPs, it is difficult to implicate which specific, if any, of these enzymes are heme-bearing. Further, collection of the venom from a snake could still involve minor trauma that could potentially result in release of heme from cytochromes from mitochondria or hemoglobin from blood cells that could then be found in the raw venom after filtration and freeze-drying. Also of concern, the amount of heme present would likely be small, and a method to detect it would need to be sensitive. Fortunately, there was an approach that addressed all these concerns.

Thus, the explicit goal of this project was to identify a fibrinogenolytic SVMP as heme modulated by CO. To achieve this goal, first a purified enzyme had to be isolated from the venom of a viper, determined to be fibrinogenolytic, and determined to be a SVMP. Second, a trypsin digest of this purified SVMP had to be analyzed with mass spectroscopy to determine if a mass consistent with heme could be identified. Lastly, it had to be determined if exposure of this heme-bearing SVMP to CO could inhibit its fibrinogenolytic activity in a well-established thrombelastographic assay (Nielsen 2018; Nielsen and Bazzell 2016, 2017; Nielsen et al. 2016, 2018a, b; Nielsen and Losada 2017; Nielsen and Matika 2017).

Materials and methods

Venom collection and processing

Trained staff performed all the experimental methods relating to the use of live animals. They observed the applicable regulations as well as institutional guidelines, according to protocols ratified by the National Natural Toxins Research Center, Texas A&M University-Kingsville, Texas, USA (Viper Resource Center at Texas A&M University-Kingsville, IACUC #: 2012–12-18A-A4) following the norms obtained from the guidelines for the care and use of laboratory animals, published by the US National Institute of Health (NIH 1985).

A Western Diamondback Rattlesnake (*Crotalus atrox*) (Avid: #009–532-076) was captured in Texas, USA. Venom was collected in the National Natural Toxins Research Center by permitting the snake to bite into Para-film (Bemis North America, Neenah, WI, USA) stretched over a disposable plastic cup. Each venom sample was centrifuged in a Beckman Avanti 30 centrifuge (Beckman Coulter, Inc., Indianapolis, IN, USA) at 10,0009×*g* for 5 min, filtered through a 0.45 μm Millipore filtration MillexHV unit (MilliporeSigma, Burlington, MA, USA) under positive pressure, and lyophilized. Venom was kept at− 90 °C until use.

Protein purification of snake venom metalloproteinase from the venom of *Crotalus atrox*

Crotalus atrox venom was fractionated by an anion-exchange chromatographic column (Waters™ DEAE 5PW, 75 × 7.5 mm, Waters Corp., Milford, MA, USA). Fractions were separated using 0.02 M Tris–HCl buffer at pH 8.0, with a 0–0.5 M NaCl gradient for 60 min, with a rate of flow of 1.0 mL/min. A Waters 2489 adjustable detector at an absorbance at 280 nm was used to monitor the proteins. Ten fractions were subjected to sodium dodecyl sulphate–polyacrylamide gel electrophoresis (SDS-PAGE). Fraction 7 contained a snake venom metalloproteinase, which was verified by N-terminal sequencing. Fraction 7 was then pooled, dialyzed in 1× phosphate buffer saline (PBS), pH 7.4, and concentrated using a 10 kDa Amicon Ultra-15 centrifugal filter (Millipore, Carrigtwohill, Ireland). The ultrafiltration on an Amicon Ultra-15 centrifugal filter was used as the second purification step and may be considered as a size exclusion separation, since it enabled clearance of the fraction of low molecular mass proteins and salts from the anion exchange chromatographic step. Purified fraction 7 was named CatroxMP-II.

SDS polyacrylamide gel electrophoresis

Seven micrograms of CatroxMP-II were electrophoresed using a precast 4–12% NuPAGE® Novex SDS-PAGE gels (Invitrogen™) in an XCell Sure-Lock™ Mini-Cell (Thermo Fisher Scientific, Waltham, MA, USA) at 100 V for 95 min. Gels were stained with SimplyBlue™ SafeStain (Thermo Fisher Scientific).

N-terminal sequencing

A 7 μg quantity of CatroxMP-II was transferred from an SDS-PAGE onto a PVDF membrane (MilliporeSigma, Burlington, MA, USA) using a Semi-Dry Transblot Cell (BIO-RAD laboratories, Inc., Hercules, CA, USA) at 125 mA for 1 h. The membrane was stained with Coomassie blue R-250 stain for 5 min and distained with 50% methanol for 5 min. The sample membrane was sent out for N-terminal amino acid sequencing at the Protein Facility, Office of Biotechnology, Iowa State University, Iowa. The identity of the primary sequence of metalloproteinase compared with other proteins was evaluated using Basic Local Alignment Search Tool (BLAST—http://blast.ncbi.nlm.nih.gov/Blast.cgi).

Fibrinogenolytic assay

The activity of CatroxMP-II was tested on human fibrinogen (Hyphen Biomed, OH, USA). Briefly, 20 μL of 5 mg/mL fibrinogen was mixed with a 10 μL of purified CatroxMP-II at various concentrations and incubated at 37 °C for 24 h. The final concentration of fibrinogen

was 3.3 mg/mL. The reactions were stopped by addition of sample denaturing buffer and analyzed by NuPAGE 4–12% Bis–Tris gel (Thermo Fisher Scientific).

The inhibition of the zinc-chelator ethylenediaminetetraacetic acid (EDTA) and the serine protease inhibitor phenylmethylsulphonyl fluoride (PMSF) on fibrinogen proteolysis by purified CatroxMP-II was investigated by incubating individual enzyme at final concentrations of 0, 100 and 300 μM of each inhibitor for 1 h at 37 °C. The mixtures were then incubated with 33 μg of fibrinogen for 24 h at 37 °C. Samples from each reaction were analyzed by NuPAGE 4–12% Bis–Tris Gel (Thermo Fisher Scientific).

For the next two phases of experimentation, the investigators at the University of Arizona purchased 20 μg CatroxMP-II in PBS at a concentration of 1 μg/mL that was received on dry ice, thawed, aliquoted into 2 μg samples, and then refrozen and maintained at− 80 °C until experimentation.

Sample digestion for mass spectrometry analysis

Trypsin (250 ng; Sigma-Aldrich, Saint Louis, MO, USA) in 20 μL of 40 mM NH_4HCO_3 was added to 1 μg of CatroxMP-II, and samples were maintained at 4 °C for 15 min prior to the addition of 50–100 μL of 40 mM NH_4HCO_3. The digestion was allowed to proceed at 37 °C overnight and was terminated by addition of 10 μL of 5% formic acid (FA). After further incubation at 37 °C for 30 min and centrifugation for 1 min, each supernatant was transferred to a clean LoBind polypropylene tube. The extraction procedure was repeated using 40 μL of 0.5% FA, and the two extracts were combined and dried down to approximately 5–10 μL followed by the addition of 10 μL of 0.05% heptafluorobutyric acid: 5% FA (v/v) and incubation at room temperature for 15 min. The resulting peptide mixtures were loaded on a solid phase C18 ZipTip (Millipore, Billerica, MA, USA) and washed with 35 μL 0.005% heptafluorobutyric acid: 5% FA (v/v) followed by elution first with 4 μL of 50% ACN: 1% FA (v/v) and then a more stringent elution with 4 μL of 80% ACN:1% FA (v/v). The eluates were combined and dried completely by vacuum centrifugation and 6 μL of 0.1% FA (v/v) was added followed by sonication for 2 min. 1 μL of the final sample was then analyzed by mass spectrometry.

Mass spectrometry and database search

HPLC–ESI–MS/MS was performed in positive ion mode on a Thermo Scientific Orbitrap Fusion Lumos tribrid mass spectrometer fitted with an EASY-Spray Source (Thermo Scientific, San Jose, CA, USA). NanoLC was performed using a Thermo Scientific UltiMate 3000 RSLCnano System with an EASY Spray C18 LC column (Thermo Scientific, 50 cm × 75 μm inner diameter, packed with PepMap RSLC C18 material, 2 μm, cat. # ES803); loading phase for 15 min at 0.300 μL/min; mobile phase, linear gradient of 1–34% Buffer B in 119 min at 0.220 μL/min, followed by a step to 95% Buffer B over 4 min at 0.220 μL/min, hold 5 min at 0.250 μL/ min, and then a step to 1% Buffer B over 5 min at 0.250 μL/min and a final hold for 10 min (total run 159 min); Buffer A = 0.1% FA/H2O; Buffer B = 0.1% FA in 80% ACN. All liquids were mass spectrometry grade. Spectra were acquired using XCalibur, version 2.3 (Thermo Scientific). A ‘‘top speed’’ data-dependent MS/MS analysis

was performed. Dynamic exclusion was enabled with a repeat count of 1, a repeat duration of 30 s, and an exclusion duration of 60 s.

CatroxMP-II exposure to CO prior to thrombelastographic analysis

In order to assess the effects of CO on CatroxMP-II activity, the following three experimental conditions were created: (1) control condition—no CatroxMP-II, DMSO 1% addition (v/v) in calcium-free PBS; (2) CatroxMP-II condition—CatroxMP-II, DMSO 1% addition (v/v) in calcium-free PBS; and, (3) CO condition—CatroxMP-II, CORM-2 (tricarbonyldichlororuthenium (II) dimer, a CO releasing molecule) 1% addition in DMSO (600 μM final concentration) in calcium-free PBS. This concentration of CORM-2 was within the range recently used to inhibit raw *C. atrox* venom (Nielsen 2018). CatroxMP-II was exposed to DMSO or CORM-2 for 5 min at room temperature. Thereafter 5 μL of one of these solutions were placed into subsequently described mixtures in a disposable thrombelastographic cup for analysis.

Thrombelastographic analyses

Sample compositions consisted of 320 μL of sodium citrate anticoagulated human plasma (George King Bio-Medical, Overland Park, KS, USA); 15 μL of calcium-free PBS, 20 μL of 200 mM $CaCl_2$, and 5 μL of one of the three aforementioned solutions containing PBS, CatroxMP-II, or CatroxMP-II exposed to CORM-2. The final solutions were placed into a disposable cup in a computer-controlled thrombelastograph® hemostasis system (Model 5000, Haemonetics Inc., Braintree, MA, USA) at 37 °C, and then rapidly mixed by moving the cup up against and then away from the plastic pin five times before leaving the mixture between the cup and pin. With regard to the concentration of CatroxMP-II used, the onset of coagulation had to be double and/or the velocity of clot formation half of plasma without CatroxMP-II addition to be acceptable for experimentation. The following elastic modulus-based parameters previously described (Nielsen 2018; Nielsen and Bazzell 2016, 2017; Nielsen et al. 2016, 2018a, b; Nielsen and Losada 2017; Nielsen and Matika 2017) were determined: time to maximum rate of thrombus generation (TMRTG): this is the time interval (minutes) observed prior to maximum speed of clot growth; maximum rate of thrombus generation (MRTG): this is the maximum velocity of clot growth observed (dynes/cm^2/second); and total thrombus generation (TTG, dynes/cm^2), the final viscoelastic resistance observed after clot formation. Data were collected for 30 min.

Data are presented as raw data or in the case of thrombelastographic data, mean ± SD. Experimental conditions in the thrombelastographic experiments were represented by n = 2 replicates per condition. A greater number of replicates or conditions for the thrombelastographic experiments for statistical analysis were deemed unnecessary as CO derived from CORM-2 has been shown to completely inhibit the fibrinogenolytic effects of unfractionated *C. atrox* venom (Nielsen 2018; Nielsen and Bazzell 2016; Nielsen et al. 2018b). Graphics were generated with commercially available programs (OrigenPro 2017, OrigenLab Corporation, Northampton, MA, USA; CorelDRAW X8, Corel Corporation, Mountain View, CA, USA).

Results

Protein purification and characterization of CatroxMP-II

Ten fractions from the *C. atrox* crude venom were procured by anion-exchange chromatography (Fig. 1). CatroxMP-II showed a single band of molecular mass of approximately 21 kDa on SDS-PAGE (Fig. 2). Its N-terminal sequence of the 12 initial residues was NPEHQRYVELFI, displaying 100% sequence homology with snake venom metalloproteinase atrolysin-e [AAB23201.1] isolated from *C. atrox* venom and metalloproteinase P-II from *Crotalus durissus durissus* [ABA42116.1], snake venom metalloproteinase Bco22 [P0DMH2.1] from *Bothrops cotiara*. CatroxMP-II at concentration of 0.25 mg/mL was able to cleave both Aα and Bβ chains of human fibrinogen at 24 h, while the γ chain was unchanged (Fig. 3a). The proteolytic activities of CatroxMP-II was fully inhibited by incubation with 100 μM of EDTA, indicating that it is metal-dependent metalloproteinase. The serine protease inhibitor PMSF had no inhibitory activity on metalloproteinase, even using the highest concentration of 300 μM (Fig. 3b). Although the remaining sequences were not determined in the partial sequencing of the CatroxMP-II from *C. atrox* venom, the N-terminal sequencing and the functional characteristics confirm that it is a P-II class metalloproteinase.

Mass spectrometry results

In order to test for the presence of heme in the CatroxMP-II sample, we analyzed 1 μg of CatroxMP-II tryptic peptide digests by ESI–MS/MS. An extracted ion chromatogram for the mass of heme in this digest (which corresponds to the singly charged m/z of heme (Jaggar et al. 2005; Nielsen et al. 2011b) revealed a peak at 101.78 min (Fig. 4, panel A, dashed arrow). This peak was confirmed to contain an ion similar to the predicted singly charged m/z of heme at 617.18 (Fig. 4, panel B, solid arrow).

Thrombelastographic results

Multiple trials with different concentrations of CatroxMP-II were conducted (0.6, 1, 2 and 5.6 μg/ mL) to establish consistent fibrinogenolytic effects in human plasma, with 5.6 μg/mL being the successful concentration. It was found that an entire 2 μg aliquot (which was how the enzyme was stored) was required for each individual 360 μL thrombelastographic sample mixture, which explains the concentration of 5.6 μg/mL. As seen in Fig. 5, plasma exposed to CatroxMP-II had increased TMRTG values (78%), decreased MRTG values (66%), and decreased TTG values (50%) compared to plasma without enzyme exposure. Exposure of CatroxMP-II to CORM-2 prior to being placed in human plasma resulted in TMRTG, MRTG and TTG values near those of plasma samples not exposed to the purified SVMP. Thus, as in the case of raw venom (Nielsen 2018; Nielsen and Bazzell 2016; Nielsen et al. 2018b), the activity of CatroxMP-II was inhibited by CORM-2 (Fig. 6).

Discussion

The present study achieved its stated goals; first, to identify and characterize a purified fibrinogenolytic SVMP; second, to detect a mass consistent with that of heme within a digest of this purified SVMP; and third, inhibit the purified, fibrinogenolytic, heme-bearing

SVMP with CO. When considered as a whole, our data support the possibility that the mechanism by which carboxyheme and metheme states inhibit the raw venoms of multiple species of snake from across the world is via modulation by the biometal, heme, attached to the various SVMP and SVSP. If true, then a new question emerges: how can heme modulation of these enzymes benefit venomous snakes?

Heme-based modulation of SVMP and SVSP activity may serve venomous snakes in a number of ways. First, if the venom gland is elaborating CO via the enzymatic action of heme oxygenase, then inhibition of SVMP and SVSP by CO is likely important in preventing these enzymes from disrupting the epithelial barrier of the gland and injuring the snake. Second, given that the body temperature of snakes tend to be between 20 and 30 °C (Raske et al. 2012; Wills and Beaupre 2000), the rate of elaboration of CO would not need to be that great to inhibit the enzymes, as the affinity of CO for heme is at its highest in this range (Saffran and Gibson 1979). Third, when a prey animal is envenomed, CO would be expected to diffuse from SVMP and SVSP and bind to the myriad of hemes found in mitochondrial cytochromes and hemoglobin in red cells perfusing the bite site. Fourth, in the case of mammalian prey such as rodents (both diurnal and nocturnal) with body temperatures of 36–37 °C (Refinetti 1996), it again would be expected that CO would bind less well to heme-bound SVMP and SVSP and quickly be released. Such rapid removal of CO from SVMP and SVSP would be analogous to ‘‘unsheathing a sword’’, allowing enzymatic action to commence and ultimately incapacitating the envenomed prey. While purely speculative at this point, such a paradigm of CO modulated enzymatic activity would be very efficient for both protection from and rapid activation of SVMPs and SVSPs used by venomous snakes. Future investigation of the various components of envenomation (e.g., venom gland heme oxygenase activity, venom CO concentration) to validate this paradigm is planned by the authors.

From a therapeutic standpoint, our data can serve as a mechanism to be exploited to potentially treat victims of venomous snakebite. Placement of carbon monoxide releasing molecules into the bite site to inhibit the action of heme-bound SVMP and SVSP may prevent in situ tissue damage and systemic coagulopathy for a period of time prior to the administration of antivenom. As carbon monoxide releasing molecules have variable CO release half-lives (Ling et al. 2017; Motterlini and Otterbein 2010), administration of a combination of quickly acting and slower release CO releasing compounds may be effective in maintaining a constant, inhibiting concentration of the gas in the envenomed tissue. Further, co-administration of a vasoconstrictor (e.g., epinephrine, phenylephrine) with CO releasing compounds could decrease exposure to circulating hemoglobin-containing red blood cells, decreasing the removal rate of CO from the bite site. All in all, it is expected that years will be required to translate this heme-based mechanism of modulation of SVMPs and SVSPs into a therapy for venomous snakebite.

In conclusion, the present work demonstrated, with diverse methodological approaches, that a novel fibrinogenolytic enzyme derived for *C. atrox* venom, CatroxMP-II, is heme-bound and inhibited by CO. Using this approach, it is hoped that other SVMP and SVSP that not only affect coagulation but that mediate tissue damage (hemorrhagins) will be investigated to determine if they are heme-bound and CO-inhibited. Lastly, it is our hope that this work

serves as the mechanistic rationale for further studies of how venomous snakes control the activity of their venom as well as further investigations to diminish injury to snakebite victims.

Acknowledgments

Funding Funding for this project was provided by the NIH/ ORIP, Viper Resource Grant 5P40OD010960–14 (NNTRC, Texas A&M University-Kingsville, Dr. E.E. Sa´nchez) and NIH/ NHLBI Grant# 1R15HL137134–01 (Dr. M. Suntravat). Additional support was provided by the Robert A. Welch Foundation Department Grant, Grant number AC-0006 (TAMUK-Department of Chemistry). We would also like to thank, Nora Diaz DeLeon and Mark Hockmu¨ ller (NNTRC Serpentarium curator) and all the NNTRC personnel. This investigation was also supported by the Departments of Medicine and Anesthesiology.

References

Jaggar JH, Li A, Parfenova H, Liu J, Umstot ES, Dopico AM, Leffler CW (2005) Heme is a carbon monoxide receptor for large-conductance Ca2 + -activated K + channels. Circ Res 97:805–812 [PubMed: 16166559]

Ling K, Men F, Wang WC, Zhou YQ, Zhang HW, Ye DW (2017) Carbon monoxide and its controlled release: therapeutic application, detection, and development of carbon monoxide releasing molecules (CORMs). J Med Chem 10.1021/acs.jmedchem.6b01153

Motterlini R, Otterbein LE (2010) The therapeutic potential of carbon monoxide. Nat Rev Drug Discov 9:728–743 [PubMed: 20811383]

Nielsen VG (2018) *Crotalus atrox* venom exposed to carbon monoxide has decreased fibrinogenolytic activity in vivo in rabbits. Basic Clin Pharmacol Toxicol 122:82–86 [PubMed: 28691277]

Nielsen VG, Bazzell CM (2016) Carbon monoxide attenuates the effects of snake venoms containing metalloproteinases with fibrinogenase or thrombin-like activity on plasmatic coagulation. MedChemComm 7:1973–1979

Nielsen VG, Bazzell CM (2017) Carbon monoxide releasing molecule-2 inhibition of snake venom thrombin-like activity: novel biochemical ‘‘brake’’? J Thromb Thrombolysis 43:203–208 [PubMed: 27787696]

Nielsen VG, Losada PA (2017) Direct inhibitory effects of carbon monoxide on six venoms containing fibrinogenolytic metalloproteinases. Basic Clin Pharmacol Toxicol 120:207–212 [PubMed: 27546530]

Nielsen VG, Matika RW (2017) Effects of iron and carbon monoxide on *Lachesis muta* muta venom-mediated degradation of plasmatic coagulation. Hum Exp Toxicol 36:727–733 [PubMed: 27488540]

Nielsen VG, Arkebauer MR, Vosseller K (2011a) Redox-based thrombelastographic method to detect carboxyhemefibrinogen-mediated hypercoagulability. Blood Coagul Fibrinolysis 22:657–661 [PubMed: 21822126]

Nielsen VG, Cohen JB, Malayaman SN, Nowak M, Vosseller K (2011b) Fibrinogen is a heme-associated, carbon monoxide sensing molecule: a preliminary report. Blood Coagul Fibrinolysis 22:443–447 [PubMed: 21451399]

Nielsen VG, Cerruti MA, Valencia OM, Amos Q (2016) Decreased snake venom metalloproteinase effects via inhibition of enzyme and modification of fibrinogen. Biometals 29:913–919 [PubMed: 27492573]

Nielsen VG, Frank N, Matika RW (2018a) Carbon monoxide inhibits hemotoxic activity of Elapidae venoms: potential role of heme. Biometals 31:51–59 [PubMed: 29170850]

Nielsen VG, Sa´nchez EE, Redford DT (2018b) Characterization of the rabbit as an in vitro and in vivo model to assess the effects of fibrinogenolytic activity of snake venom on coagulation. Basic Clin Pharmacol Toxicol 122:157–164 [PubMed: 28696521]

Raske M, Lewbart GA, Dombrowski DS, Hale P, Correa M, Christian LS (2012) Body temperatures of selected amphibian and reptile species. J Zoo Wildl Med 43:517–521 [PubMed: 23082515]

Refinetti R (1996) Comparison of the body temperature rhythms of diurnal and nocturnal rodents. J Exp Zool 275:67–70 [PubMed: 8708632]

Saffran WA, Gibson QH (1979) The effect of temperature on carbon monoxide binding to a root effect hemoglobin. J Biol Chem 254:1666–1670 [PubMed: 762165]

Wills CA, Beaupre SJ (2000) An application of randomization for detecting evidence of thermoregulation in timber rattlesnakes (*Crotalus horridus*) from northwest Arkansas. Physiol Biochem Zool 73:325–334 [PubMed: 10893172]

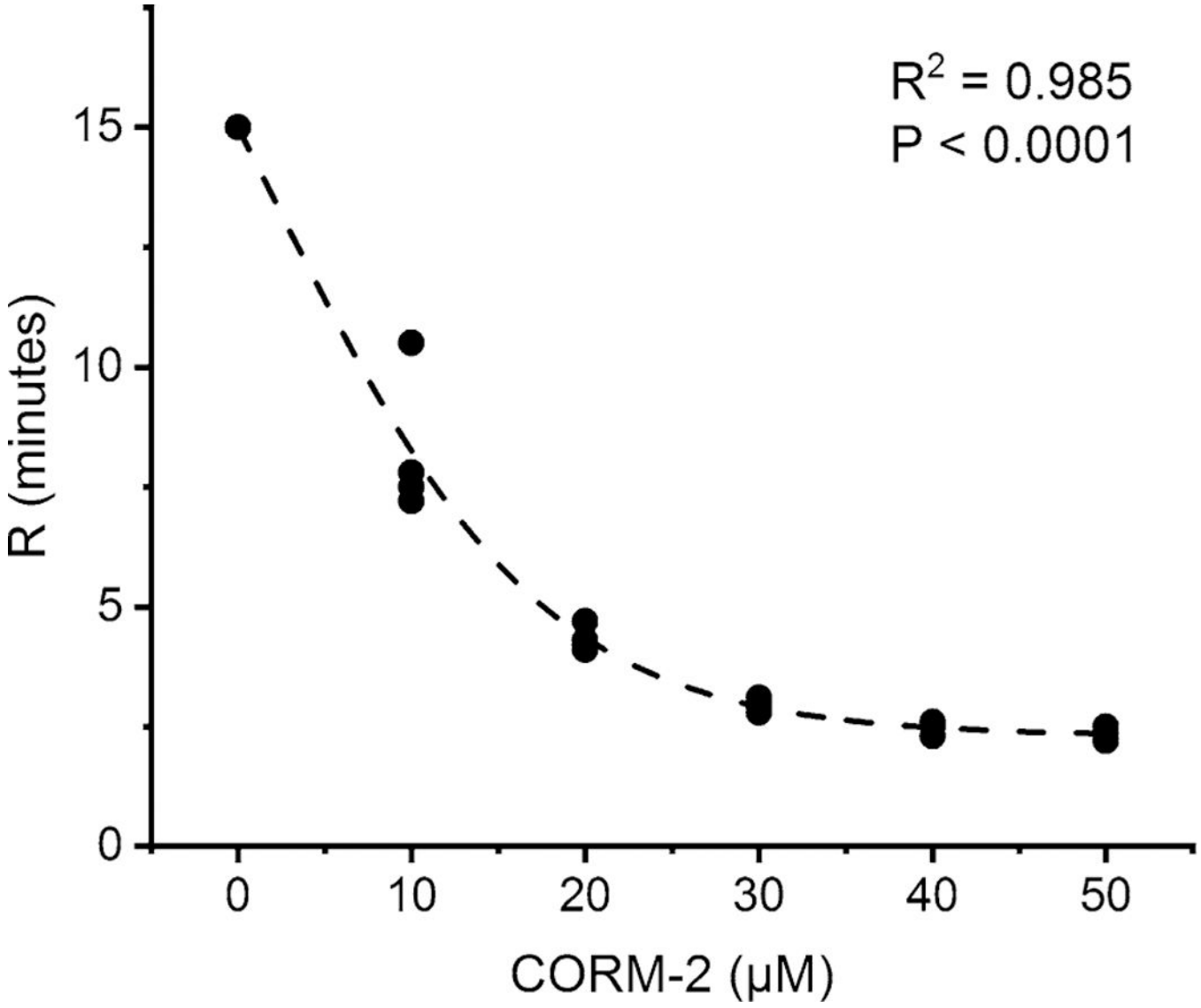

Fig. 1.

Thrombelastographic demonstration of CO concentration-coagulation kinetic response of fibrinogenolytic activity of raw *Crotalus atrox* venom exposed to CORM-2. Each concentration of CORM-2 is represented by four different exposures of venom prior to being placed in human plasma. Reaction time (R, min) is defined as the time to reach an amplitude of 2 mm in a thrombelastographic sample; it is considered the beginning of coagulation. As CORM-2 (tricarbonyldichlororuthenium (II) dimer, a CO releasing molecule) concentration (μM) increased, R values decreased as the fibrinogenolytic effects of the venom decreased. The fitted model is sigmoidal (Boltzmann), with P value and coefficient of determination (R^2) displayed. This data, previously unpublished, was generated from samples published elsewhere (Nielsen and Bazzell 2016). The fitted equation describing this association was: R (min) = $25.04/1 + e^{(([CORM-2]-1.83)/7.84)}$

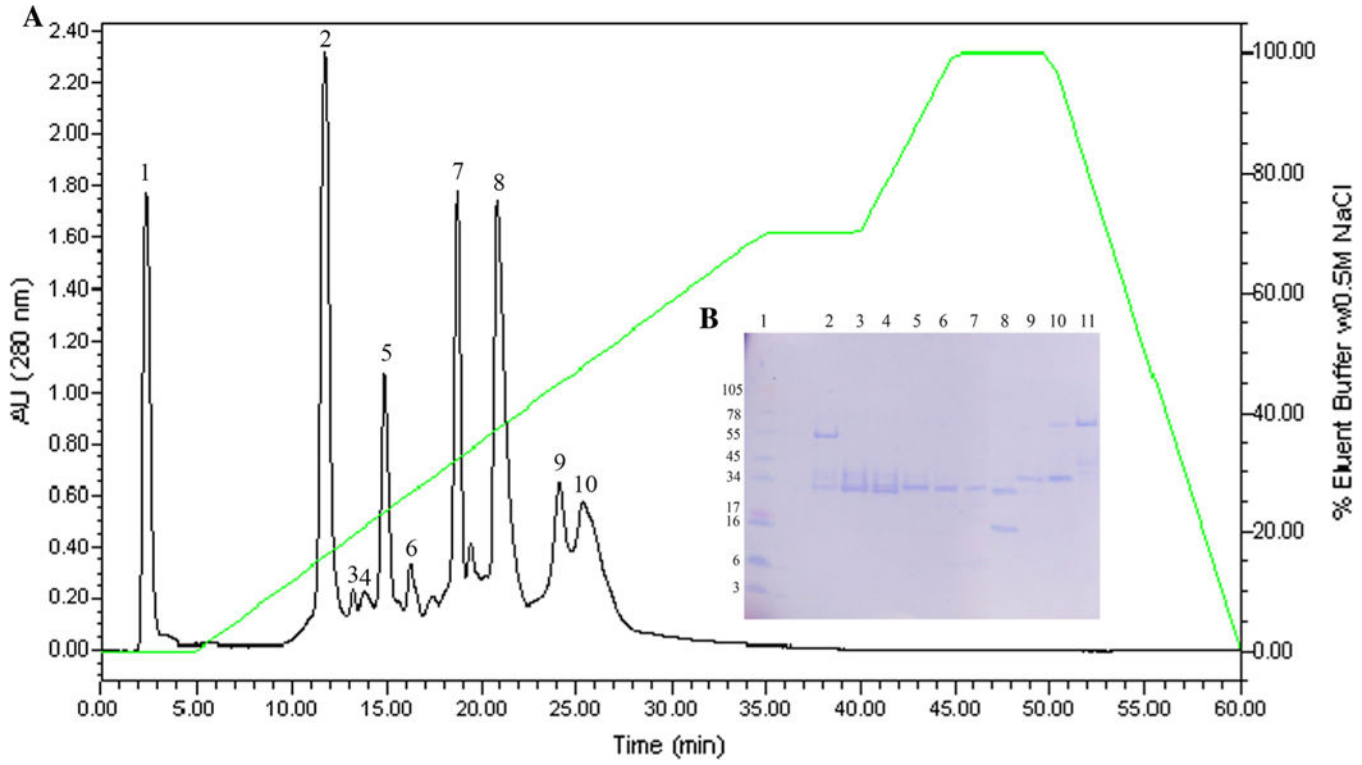

Fig. 2.

Purification of CatroxMP-II. **a** DEAE anion exchange HPLC profile of crude *C. atrox* venom. **b** SDS-PAGE analysis of *C. atrox* venom fractions from C18 DEAE anion exchange HPLC. Venom fractions (10 μg) were run on 10–20% Tricine SDS-PAGE under non-reducing condition at 125 V for 90 min. Lane 1: SeeBlue Plus2 Markers; lanes 2–11: venom fractions 1–10, respectively

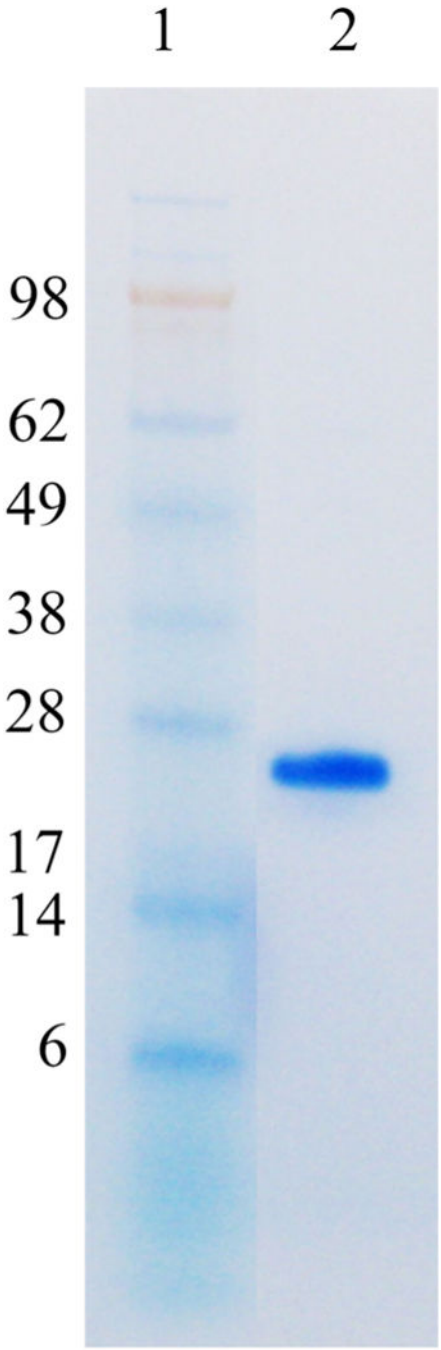

Fig. 3.

SDS-PAGE of purified CatroxMP-II from the venom of *C. atrox*. Samples were run on 4–12% Bis–Tris Gel under non-reducing conditions at 100 V for 95 min. The gel was stained with RapidStain. Lane 1: SeeBlue Plus2 Markers; lane 2: purified CatroxMP-II (8 μg)

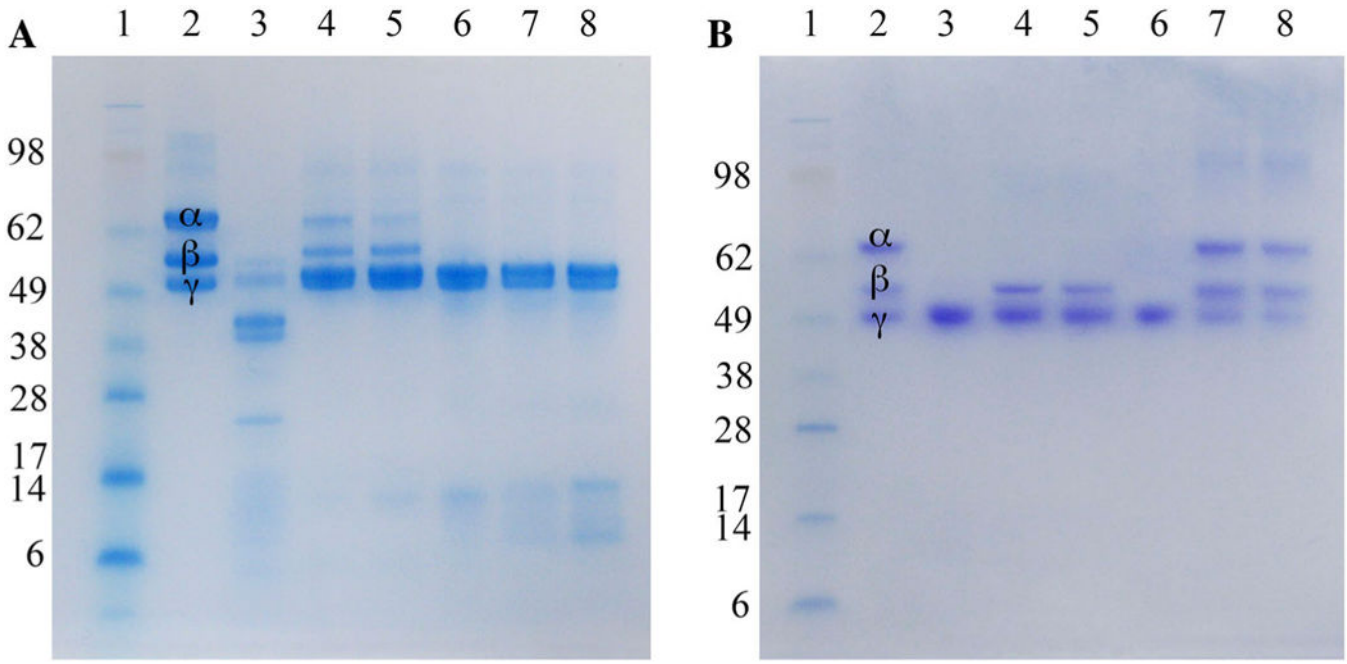

Fig. 4.

Fibrinogenolytic activity of CatroxMP-II. **a** SDS-PAGE of human fibrinogen when mixed with purified metalloproteinase at various concentrations. Human fibrinogen premixed with an equal volume of purified CatroxMP-II at various concentrations (0.05, 0.1, 0.25, 0.5, and 1 mg/mL) for 24 h at 37 °C were run on a 4–12% Bis–Tris SDS-PAGE gel under reducing conditions at 100 V for 95 min. Gel was stained with RapidStain. Lane 1: SeeBlue Plus2 Markers (InvitrogenTM); lane 2: human fibrinogen; lane 3: human fibrinogen mixed with crude *C. atrox* venom; lanes 4–8: human fibrinogen mixed with purified CatroxMP-II at 0.05, 0.1, 0.25, 0.5, 1 mg/mL, respectively. **b** Inhibition of CatroxMP-II-mediated proteolysis of fibrinogen. The same experiment conditions as described in Fig. 3, Panel A, but addition of EDTA or PMSF at different concentrations and incubated for 24 h at 37 °C. Samples were run on a 4–12% Bis–Tris SDS-PAGE gel under reducing conditions at 100 V for 95 min and Coomassie blue stained. Lane 1: SeeBlue Plus2 Markers (InvitrogenTM); lane 2: human fibrinogen; lanes 3–5: CatroxMP-II pre-mixed with 0, 100, 300 μM PMSF; lanes 3–5: CatroxMP-II pre-mixed with 0, 100, 300 μM EDTA

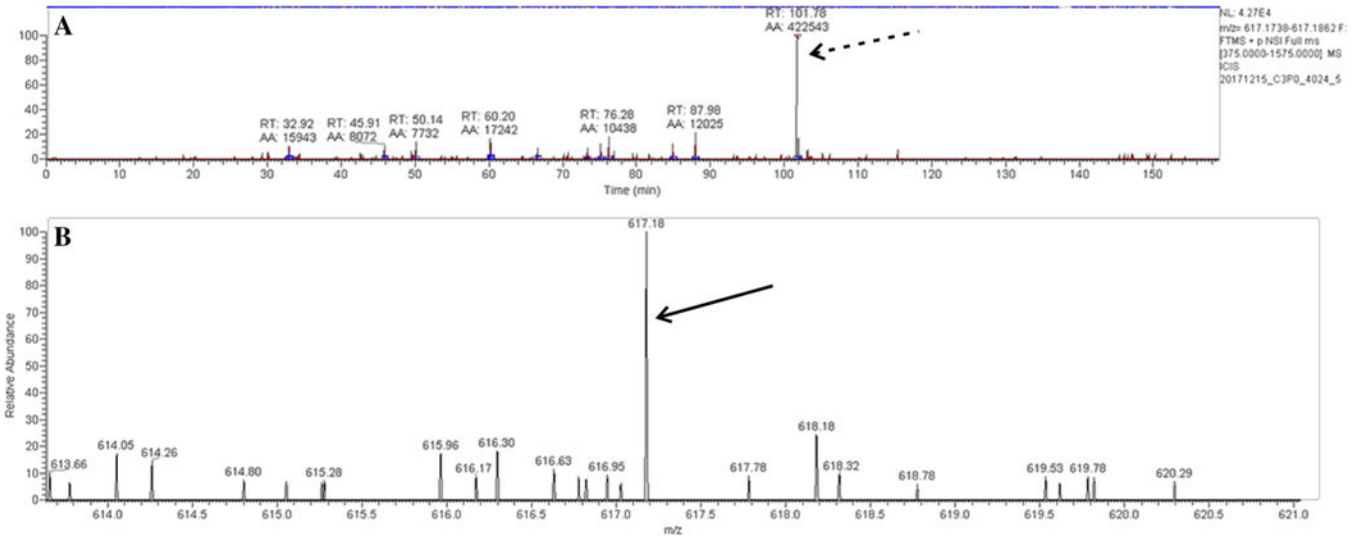

Fig. 5.

Mass spectrometry results. **a** An extracted ion chromatogram for the mass of heme in this digest revealed a peak at 101.78 min (dashed arrow). **b** This peak was confirmed to contain an ion similar to the predicted singly charged m/z of heme at 617.18 (solid arrow)

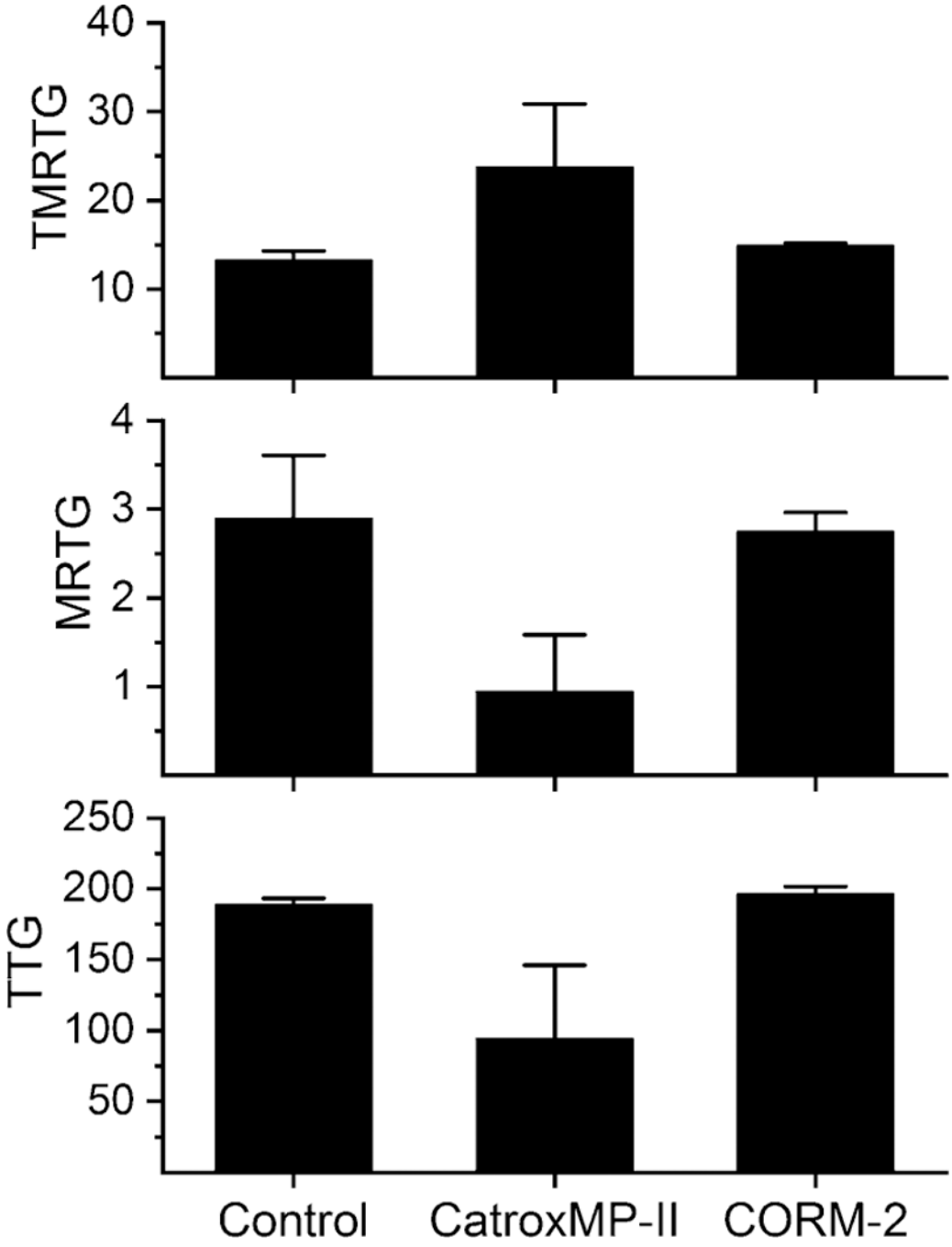

Fig. 6.

Thrombelastographic results of addition of CatroxMP-II to human plasma without or with CORM-2 pre-exposure. Data are presented as mean ± SD, with n = 2 per condition. Control = no additives; CatroxMP-II = 5.6 μg/mL of the enzyme present; CORM-2 = 5.6 μg/mL CatroxMP-II exposed to 600 μM CORM-2. *TMRTG* time to maximum rate of thrombus generation (minutes), *MRTG* maximum rate of thrombus generation (dynes/cm^2/second), *TTG* total thrombus generation (dynes/cm^2)